INFLUENCE OF STRAIN RATE AND SOLIDIFICATION RATE ON MECHANICAL BEHAVIOUR OF AL-SI-MG ALLOYS

J.L. Douziech*, C. Berdin*, R. Doglione**, D. François*

This study concerns the elastic-viscoplastic behaviour and fracture of a chill and a sand cast aluminium-silicon alloy. Classical uniaxial static tests and hopkinson's bars tests in compression as well as in tension have been performed on both materials. A classical logarithmic law is found for the elastic-viscoplastic behaviour within the considered range of strain rates. The fracture strain increases with strain rate and with solidification rate. An analysis of these results is made in the light of physical damage mechanisms for these materials.

INTRODUCTION

Cast aluminium alloys are now being used more frequently for safety components in the automotive industry because of improved manufacturing procedures. In order to assess the behaviour of a safety component under crash conditions, it is necessary to evaluate the material's behaviour under high speed loadings. There are some general studies on the strain rate sensitivity of metallic materials (1) (2), but none for cast Al-Si-Mg at intermediate to high strain rates ($< 10^3 s^{-1}$) which correspond to a crash situation, providing information about the strain rate sensitivity of ductility. This work deals with the study of strain rate-sensitivity of a Al-Si-Mg alloy, obtained with two different castings methods : sand and chill casting. Relationships between macrostructure and mechanical properties are outlined.

* Laboratoire de Mécanique des Sols, Structures et Matériaux,CNRS 850, Ecole Centrale de Paris, Grande Voie des Vignes, F92295 Châtenay Malabry cedex, France
** Dipartimento di Scienza dei Materiali e Ingegneria Chimica, Polticenico di Torino, cs.o Duca degli Abruzzi 24, 10129 Torino, Italy

MATERIAL AND EXPERIMENTAL PROCEDURES

Material. This study was conducted on a AS7G03 alloy (AFNOR standard) which is equivalent to A 356 (ASTM standard). It is a hypo-eutectic aluminium alloy with 7 wt%Si, 0.3 wt%Mg (3). This alloy is submitted to a heat treatment, which consists in a water quench after 6h at 560°C, and a temper of 6h at 160°C. This alloy is modified with Na in order to improve the ductility. Two types of casting were used, sand and chill castings, so as to achieve very different solidification rates with a ratio around 10. The microstructure, figure 1, consists of primary dendrites of Al, strengthened by Mg_2Si precipitates and a eutectic phase. A quantitative metallographic study (3) concludes that there is no noticeable difference in size and shape for the Si particles in the two castings. However the spatial distribution of the eutectic phases, and thus the dendrite size is very different for the two solidification rates : the mean interdendritic spacing is 100% higher in the sand than in the chill casting (3).

Experiments. Classical uniaxial tests were performed in tension and in compression with mechanical (Instron) and hydraulic (M.T.S.) machines, for static and intermediate strain rates ($< 100s^{-1}$). For the higher strain rates, a Hopkinson's bars apparatus was used, to perform classical compressive tests and tensile tests using Ogawa's method (5). All tests were conducted at room temperature and load versus displacement was registered, except for the Hopkinson's bars, where the strains of the incident and transmission bars lead to the definition of the material behaviour law (6). Table 1 summarises the tests conditions.

Sand casting		Chill casting	
tension ($\dot{\varepsilon}$)	compression ($\dot{\varepsilon}$)	tension ($\dot{\varepsilon}$)	compression ($\dot{\varepsilon}$)
0.02	0.02	0.02	0.02
560	950	8 560	950

Table 1. Strain rates used for mechanical tests (s^{-1}).

RESULTS

The true stress versus the logarithmic strain are given in the figures 2-3 for chill and sand castings. The compression curves are plotted until 15% deformation only, since deformation becomes inhomogeneous beyond this point, and the samples become barrel shaped. The compression tests are used to obtain the strain rate sensitivity, and the tensile tests lead to the determination of the fracture strain. It should be noted that for tensile tests using Hopkinson's bars, the load is somewhat underestimated because of the assumptions made in analysing the data regarding to the propagation of the stress wave (7). The peak in stress observed at high rate is caused by the presence of a gap between the thread of the sample and the inner thread of the fixture.

There is no difference of mechanical behaviour between tension and compression. Considering all tests as isothermal, it is essentially the yield stress and not the strain hardening wich is sensitive to the strain rate. Nevertheless this sensitivity is weak. The fracture strain of sand casting is less than that of the chill casting for the static case. In increasing the strain rate, the fracture strain increases as well, but it seems that the difference observed in static case between sand and chill castings, is reduced.

DISCUSSION

It is known from the litterature (2-3-8) that for commercially pure aluminium and for Al-based solid solutions (e.g. A. 6061-T6), the flow stress follows a linear dependence on the logarithm of the strain rate, at least up to 10^3 s^{-1}, Figure 4. Marked increase in the strain rate sensitivity is reported for extremely high rates, above 10^3 s^{-1}, which have not been explored here. The results presented in this paper follow this classical linear dependence. This behaviour is not surprising, since the flow properties of the AS7G03 alloy are mostly governed by the aluminium strengthened matrix phase, and thus they are fully comparable to those of A 6061-T6. The eutectic silicon particles present in the AS7G03 alloy essentially play a role in the damage process of the material (3). The strain sensitivity of the alloy is therefore attributed to the rate at which the thermally activated dislocations cut the forest dislocations. Since total dislocation density increases with strain rate, it is expected that the material behaviour be independent on casting technology. This is confirmed by the fact that, in spite of the very different eutectic distribution (Figure 1), chill and sand castings show the same trend of the flow stress versus strain rate.

The evolution of fracture strain with strain rate has long been associated with that of steel, where the strain to fracture is lowered when the strain rate is increased. However, it is now currently accepted that, for aluminum alloys, tensile ductility can increase with strain rate, as is observed in figures 2b-3b. It has been reported that no significant change in the strain at maximum-load is usually noticed, and that the increase in total strain is due primarily to an increase of post uniform elongation. This fact has been related to inertia effects (9). However, negligible striction has been observed at all strain rate conditions on our samples. Moreover, since it is known that inertial effects scale with material density, which is quite low in our case, and strain rate sensitivity, which is again low, increase in tensile strain with strain rate should be minimal in AS7G03 alloy. This behaviour is verified within experimental error for chill casting specimens, as observed in figure 2b. On the other hand, sand castings show an increase in elongation up to the value characteristic for chill castings, figure 3b. We propose that this effect is linked to the damage process of these alloys. Static damage and failure mechanism were determined by in-situ experiments, reported in Ref.(3), and are briefly recalled in what follows. In hypo-eutectic Al-Si alloys, damage is the result, upon straining, of rupture and decohesion of eutectic Si particles, and subsequent nucleation and growth of microcracks in the solidified eutectic. Even if the final fracture is typically ductile with dimples corresponding to the broken Si particles, no void growth and coalescence is observed. Rather, failure is produced by the propagation and linking of microcracks in the eutectic phase, the enhanced strain in chill castings resulting from branching of the crack path related to the eutectic distribution (Figure 1). At high strain rates, post-mortem fractographic studies have not shown any substantial variations in the fracture mechanisms, and in particular no change in dimple size was noticed. The explanation proposed in Refs.(10) and (11), which postulates an increase in dimple size and a delay in void coalescence to account for the increase in strain, can therefore not be invoked in our case . We would rather agree with the suggestion proposed in Ref (12), namely that dynamic loading in general favours the spreading of the damage because the rate of nucleation of microcracks is increased and the time for microcracks to grow is reduced, thus reducing localization of strain. In the case of AS7G03-Y33 alloy, this occurs at quasistatic strain rates for chill casting, owing to its distribution of eutectic phase. At high strain rates no substantial variation in damage distribution arises, thus justifying the minimal variation in fracture strain. The opposite occurs in sand castings, where an increase in strain rate multiplies and spreads damage sources, leading to a rise in

ductility. This explanation is comforted by the fact that during Hopkinson bar testing, stress waves may induce some non-uniformity in load, enhancing diffuse microcrack nucleation in sand casting.

CONCLUSION

Tension and compression tests performed on the AS7G03 casting alloy aged at the hardness peak in the strain range between 10^{-3} and 10^{3} s^{-1} have showed that the elastic-viscoplastic behaviour follows a linear increase of the flow stress with the logarithm of the strain rate. The fracture strain shows a slight increase for chill castings, whereas for sand castings the increase is larger. The reasons of this behaviour were discussed taking into account the distribution of the eutectic solid. It is concluded that, owing to the negligible necking in the tested strain rate range, inertia effects have little influence on the ductility, and enhanced fracture strain in sand casting is attributed to more diffused damage nucleation with increasing strain rate.

ACKNOWLEDGEMENTS

Mr. Douziech acknowledges financial support from PSA. Mr Doglione was working with the support of a HCM fellowship of EEC. Thanks are due to Mr Rémillieux, Mr. Diani, Mr. Clisson and Mr. Longere of Établissement Central de l'Armement for use of their facilities, and helpful discussions.

REFERENCES

(1) Tirupataiah, Y., Sundararajan, G., "The Strain rate sensitivity of Flow Stress and Strain Hardening rate in Metallic Materials", Mat. Sc. Eng. vol.A189, 117-127, 1994.

(2) Sapounov, V.T., Morozov, E.M., Azari, Z., Pluvinage, G., "Déchirement ductile en statique et dynamique des alliages d'aluminium", Revue Française de Mécanique, vol.3, 239-244, 1994.

(3) Doglione, R., Douziech, J.L., Berdin, C., François, D., "Microstructure and Damage Mechanisms in A356-T6 Alloy", ICAA-7, Grenoble (France), 1-3 july 1996.

(4) Roudier P., "Contribution à l'étude de la vitesse de sollicitation sur le comportement à rupture d'alliage de Titane", Thése , 1994.

(5) El-Magd, E., "Mechanical Properties at High Strain Rates", Eurodymat 94, Oxford (UK), sept. 1994.

(6) Bertholf, L.D., Karnes, H., "Two-dimensional Analysis of the Split Hopkinson Pressure Bar System" J. Mech. Phys. Solids, vol. 23, p. 1-20, 1973.

(7) Caceres, C.H., Davidson, C.J., Griffiths, J.R., "The Deformation and Fracture Behaviour of an Al-Si-Mg Casting alloy", Mat. Sc. Eng., vol.A197, 171-179, 1995.

(8) Xiaoyu, Hu, Robert, H.W., Glenn, S.D., Somnath, G., "The Effect of Inertia in Tensile Ductility", Met. Mat. Tr. A, vol.25A, 2723-2735, 1994.

(9) Mukai, T., Higashi, K., Tanimura, S., Mat. Sci. Eng., A 176, p. 181, 1994.

(10) Worswick, M.J., Nahme, H., Clarke, J., Fowler, J., Dymat J;, Vol. 1, nr 3, p. 229, 1994.

(11) Rao, K.V., Lee, K.H., Polonis, D.H., Mat. Sci. Eng., 92, p. 91, 1987.

(12) Ansart, J.P.,"Loi de comportement", stage ENSTA/DYMAT M10, p. 10, 1990.

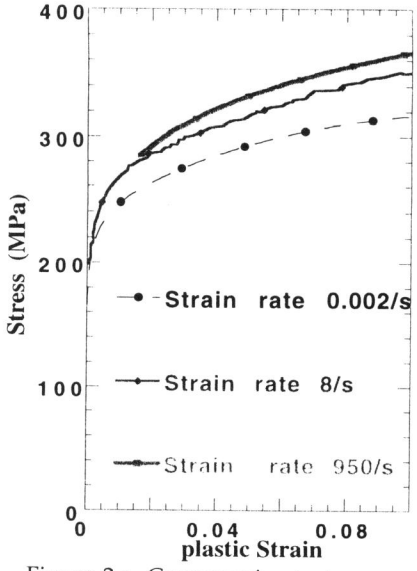

Figure 2.a. Compressive tests.

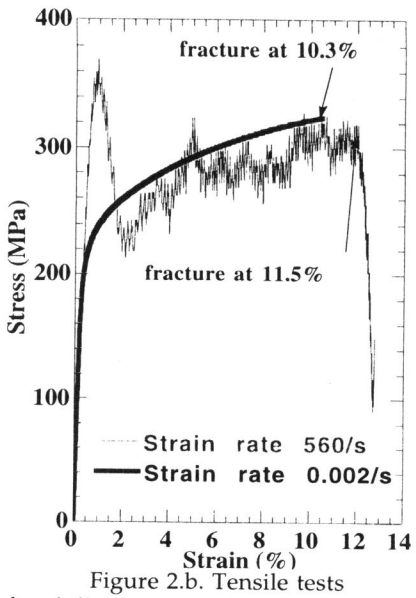

Figure 2.b. Tensile tests

Figure 2. Stress-strain curves for chill casting.

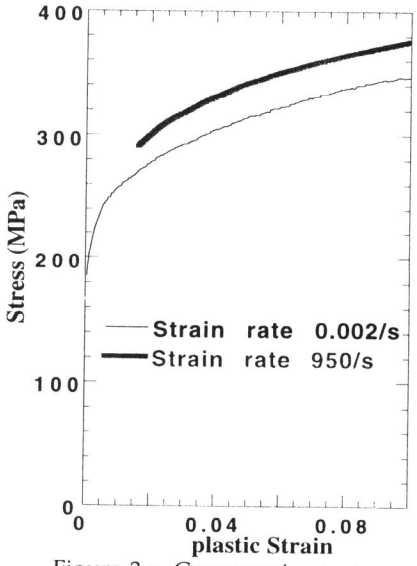

Figure 3.a. Compressive tests.

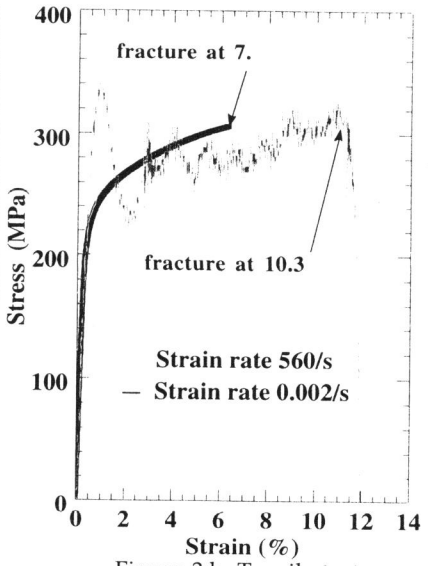

Figure 3.b. Tensile tests

Figure 3. Stress-strain curves for sand casting.

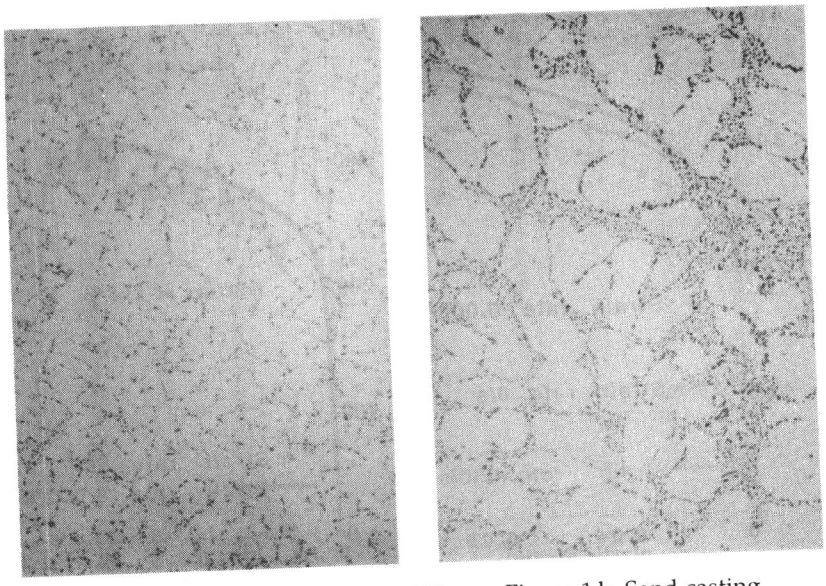

Figure 1.a . Chill casting. ⟵⟶ 100μm Figure 1.b. Sand casting.
Figure 1. Micrographies of the aluminium alloy.

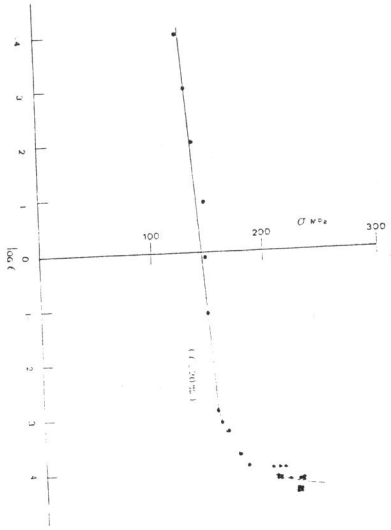

Figure 4 . Stress vs. strain rate for
aluminium at 20% of strain from ref.12